

Carbon Star Populations in Systems with Different Metallicities: Statistics in Local Group Galaxies.

M. Mouhcine, A. Lançon

Observatoire Astronomique de Strasbourg (UMR 7550), 11, rue de l'Université, 67000 Strasbourg, France.

Accepted ?. Received ?; in original form ?

ABSTRACT

We present evolutionary population synthesis models for the study of the cool and luminous intermediate age stellar populations in resolved galaxies with particular emphasis on carbon star populations. We study the effects of the star formation history, the age and the metallicity on the populations of intermediate mass stars. In the case of instantaneous bursts, we confirm that lower metallicity results in higher contributions of carbon stars to the total star number, and in higher number ratios of carbon stars to late-type M stars.

Chemically consistent models are used to study the effect of the star formation history on the relations between carbon star population properties and global parameters of the parent galaxy (age, metallicity). Our models are able to account, for the first time, for those correlations, as observed in the galaxies of the Local Group. For stellar populations older than about 1 Gyr, the properties of carbon star populations are linked to the current metallicity in a way that is quite independent of the star formation scenario. The number ratio of carbon stars to late-type M stars forms a metallicity sequence along which stellar populations with very different star formation histories are found.

For the same populations, we find that both the mean bolometric luminosity of carbon stars and their normalized number to the luminosity of the parent galaxy are quite independent of metallicity over a large range in metallicity. This is in good agreement with the observational constraints.

The observed statistics of carbon star populations can be interpreted by two principal effects: (i) the carbon star formation efficiency is higher in metal-poor systems, (ii) the typical star formation timescale along the Hubble sequence of galaxies is much longer than the typical timescale for the production of carbon stars at any metallicity.

Key words: stars: AGB - stars: carbon - stars: evolution - stars: mass loss - galaxy: dwarf, morphology

1 INTRODUCTION

The stellar content of galaxies has long been recognized as holding important clues to the understanding of the formation and the evolution of galaxies. Better understanding of galaxy evolution in terms of stellar populations and chemical evolution requires knowledge of the Asymptotic Giant Branch (AGB) stars. From a purely pragmatic point of view, the evolved AGB stars are easy targets to observe in external galaxies even far beyond the Local Group, and to segregate from the bulk of the stellar population: they are red and luminous sources. Stars in the AGB phase make a significant contribution to the integrated light of a stellar population (Frogel et al. 1990). Mouhcine & Lançon (2002) estimate that the thermally pulsing AGB stars (TP-AGBs) are responsible for 30–60% of the integrated JHK luminosities of a system whose stars are 0.2–2 Gyr old, with a maximum contribution at ~ 0.8 –1 Gyr. Those properties make AGB stars useful tools to get information on the star forma-

tion (SF) history, even through several magnitudes of absorption (Hodge 1989). Due to their large luminosities, carbon stars of the AGB are used as tracers of kinematics to probe morphological and kinematical structures (Aaronson & Olszewski 1987, Hardy et al. 1989, Kunkel et al. 1997, Graff et al. 2000).

Stars in the AGB phase are classified as either oxygen rich ($C/O < 1$ by number) or carbon rich ($C/O \geq 1$). Spectra of oxygen rich stars are dominated by metal oxide bands such as TiO, VO, and H₂O whereas carbon stars have bands of C₂ and CN (Barnbaum et al. 1996, Joyce 1998). Using those features, groups led by Richer (Richer et al. 1984, Richer et al. 1985, Pritchett et al. 1987, Hudon et al. 1989), Aaronson and co-workers (Aaronson et al. 1982, Aaronson et al. 1984, Cook et al. 1986, Aaronson et al. 1985, Cook & Aaronson 1989) developed a technique to identify AGB stars and to determine their nature in crowded fields. This technique involves imaging a field through four filters. Two narrow-band filters provide spectral information on the CN and TiO bands

(Wing 1971), while broad-band colours provide information on the effective temperature of the stars, and can discriminate between early type and late-type stars. Extensive observational work, using this technique and others (Frogel & Richer 1983, Azzopardi et al. 1985, 1986, 1998; Azzopardi & Lequeux 1992; Westerlund et al. 1987, 1991 a & b, 1995; Demers et al. 1993, Battinelli & Demers 2000) has lead to the identification and classification of AGB stars in nearby galaxies. Recent comprehensive compilations of late-type stellar contents, and of their systematic statistics, can be found in Mateo (1998), Groenewegen (1999) and Azzopardi (2000).

In order to interpret those findings, we have developed a chemically consistent population synthesis model that includes the various phenomena relevant to the production of carbon stars, and their dependence on metallicity. We use it to evaluate, qualitatively and quantitatively, (i) the interplay between different physical processes that operate during the AGB phase and control the formation of carbon stars, (ii) how these processes lead to the observed statistics of carbon star populations in the galaxies of the Local Group, and (iii) the sensitivity of the carbon star statistics on the global properties of the host galaxies (SF history, evolutionary status). The paper is organized as follows. In Section 2 we present our current observational knowledge of the statistics of carbon star populations in the Local Group. In Section 3, we describe the calibrated semi-analytical evolution models that we use to follow the evolution of the TP-AGB stars. We also describe the population synthesis and the chemical evolution models. In Section 4 and 5, we present the predicted statistics of carbon stars for single stellar populations (SSPs) and address the effect of opaque dust envelopes on those statistics. In Section 6 we calculate the statistics for continuous SF histories representative of various morphological types, and compare our results with the observational data. In Section 7, we come back to the use of the relative number of carbon stars as an abundance indicator. The conclusions are summarized in Section 8.

2 OBSERVATIONAL STATISTICS AND CONSTRAINTS

2.1 The number ratio of carbon stars to late type M stars

Large sets of observational data on resolved galaxies clearly show that the number ratio of carbon stars to late type M stars, N_C/N_M , depends on metallicity, in the sense that higher ratios are observed in lower metallicity environments (Blanco & McCarthy 1983, Richer et al. 1985, Cook et al. 1986, Mould & Aaronson 1985, Aaronson et al. 1987, Brewer et al. 1996, Albert et al. 2000). Even though large observational uncertainties affect metallicity and N_C/N_M measurements (about 0.2 dex for $[\text{Fe}/\text{H}]$ and 50% for N_C/N_M ratio), and although different carbon star surveys have covered different fractions of the area of the target galaxies with different completeness limits, the N_C/N_M vs. $[\text{Fe}/\text{H}]$ correlation is well established (Groenewegen 1999). The observed sequence spans over a wide range in metallicity and N_C/N_M (1.5 dex in $[\text{Fe}/\text{H}]$ and 4 dex in N_C/N_M). The most striking feature of this sequence is that galaxies with different morphologies and different carbon star luminosity functions, indicating different SF histories, lie on the same sequence. This behavior suggests that the parent galaxy metallicity is the predominant factor, in comparison to age, in determining the observed ratio.

Two arguments have been developed qualitatively in the literature to explain this effect. The first one is related to the effect of metallicity on the effective temperature of the giant branch. It leads to larger numbers of late type M stars in metal-rich systems. The

second one is a more efficient mixing of carbon from the stellar core into the atmosphere in low-metallicity stars. However, those qualitative arguments must be viewed with some caution, since the SF history may also play some role in determining the relative frequency of carbon and M stars in galaxies.

2.2 The mean bolometric luminosity of carbon rich stars

The determination of the mean bolometric luminosity of the whole carbon star population is sensitive to distance determination, survey completeness limits, or surface coverage of the galaxy. Rapid examination of the data (Fig. 6 of Groenewegen 1999, or Fig. 9b of Aaronson & Mould 1985) can lead one to find an anticorrelation between the mean bolometric magnitude of carbon star populations and the metallicity. However, some caution must be exerted. Carbon stars in Ursa Minor or Draco for example, lie below the giant branch tip in the colour-magnitude diagram (Aaronson & Mould 1985). They may not be on the AGB. Indeed there are two possible origins of these faint carbon stars (see also Sect. 3.2.3). The first one is that we are seeing dwarf carbon stars (i.e. not AGB stars), enriched in carbon by mass transfer from a companion. The second possibility is that we are looking at carbon stars on the AGB, but evolving through the luminosity dip that follows a thermal pulse. The second possibility is unlikely when *only* carbon stars fainter than the tip of the red giant branch are found, as the luminosity dips represent a small fraction of the thermal pulse cycle: carbon stars with magnitudes consistent with the AGB core mass-luminosity relation should also be present (see Sect. 3).

If one considers only those stellar populations whose carbon stars are in the AGB phase, the derived mean bolometric luminosity of the carbon star population seems to be constant and equal to ≈ -4.7 over a large range of metallicities. This observational fact was reported in the literature since the beginning of the 80's. Aaronson & Mould's data (1985) support this result. Richer et al. (1985) concluded that as long as a galaxy is relatively metal rich ($[\text{Fe}/\text{H}] > -1.8$), its carbon stars will have the same mean bolometric luminosity as those of Fornax, the Magellanic Clouds, the Milky Way, M31, and NGC 205. Brewer et al. (1996) observed different fields in M31, and they also derived that all have the same mean bolometric luminosity.

One has to keep in mind that the universal quantity is the mean bolometric luminosity of the whole AGB carbon star population, not the carbon star luminosity function. The bright tail of the luminosity function is sensitive to recent star formation episodes (Marigo et al. 1999).

2.3 The luminosity-normalized number of carbon stars

The third statistical property of carbon star populations is the behavior of the luminosity-normalized number of carbon stars as a function of galaxy metallicity. This quantity is a measurement of the number of carbon stars per V-band (or sometimes B-band) luminosity unit, grossly equivalent to a number of carbon stars per mass unit (Aaronson et al. 1983, Aaronson & Mould 1985). We define $\log N_{C,L} = \log N_{\text{Tot},C} + 0.4 M_V$, where $N_{\text{Tot},C}$ is the total number of carbon stars and M_V the integrated absolute V band magnitude of the whole population. $N_{C,L}$ is of interest because it gives a possibility of deriving constraints on the physical processes that control the formation of carbon stars.

The observational determinations of this quantity suffer from the uncertainties in the surface photometry, internal absorption,

possible incompleteness, and errors on distance determinations. Most of the observational determinations of $\log N_{C,L}$ scatter between a value of -3 and -4 up to $[\text{Fe}/\text{H}] \approx -0.5$. For higher metallicities, there is a large dispersion in $N_{C,L}$ at constant metallicity, with evidence for a trend of decreasing $N_{C,L}$ for increasing $[\text{Fe}/\text{H}]$. Azzopardi et al. (1999) noted that on average $\log N_{C,L} \simeq -3.3$ for Local Group galaxies over a large range in magnitude (or metallicity). Draco, Ursa Minor and Carina stand out with large empirical values of $N_{C,L}$ but, as mentioned in Sect. 2.2, the carbon stars in those galaxies may not be in the AGB phase. The observed behavior appears to exclude the interpretation of the N_C/N_M vs. $[\text{Fe}/\text{H}]$ relation as due only to the effect of the metallicity on the effective temperature of the red giant branch. The relative insensitivity of $N_{C,L}$ to metallicity suggests that the *total* number of carbon stars scales with the parent galaxy magnitude, and consequently with the galaxy metallicity.

3 EVOLUTIONARY MODELING

3.1 Stellar population models

Our calculations are based on the stellar evolutionary tracks of the Padova group (Bressan et al. 1993, Fagotto et al. 1994 a,b). For intermediate age stars, these tracks do not include TP-AGB phase. We include that phase with new synthetic evolution models for metallicities $[Z=0.0004, Y=0.23]$, $[Z=0.004, Y=0.24]$, $[Z=0.008, Y=0.25]$, $[Z=0.02, Y=0.28]$, and $[Z=0.05, Y=0.352]$. In the following subsections, we highlight only the most important physical processes that affect the behavior of the TP-AGB stars in the HR diagram and their chemical nature, as it was pointed out with detailed structural models (Boothroyd & Sackmann 1992, Blöcker & Schönberner 1991, Frost et al. 1998, Wagenhuber & Tuchman 1996). Synthetic evolution models account for these effects with analytical formulae derived from full numerical calculations, and will remain an attractive tool as long as large enough grids of complete models for the structural evolution of TP-AGB stars stay out of reach (Iben & Truran 1978, Renzini & Voli 1981, Groenewegen & de Jong 1993, Marigo et al. 1996). Complementary information on our models is given by Mouhcine & Lançon (2002), who focused on the integrated spectrophotometric evolution of intermediate age populations at the metallicities of the solar neighborhood and the Magellanic Clouds.

The assumptions on which TP-AGB evolution models stand are motivated mainly by the ability of their predictions to reproduce the observations of simple stellar populations. Mouhcine & Lançon (2002) and Mouhcine et al. (2002) show that the adopted ones adequately reproduce the emission properties of star clusters. Here, our principal goal is to study resolved carbon star populations, and the sensitivity of their properties to star formation history and chemical evolution of galaxies.

3.2 TP-AGB evolution models

3.2.1 Dredge-up and Hot Bottom Burning

The third dredge-up is of crucial importance for the formation of carbon stars. The adopted semi-analytical treatment of this process requires the knowledge of three inputs: (i) the critical core mass M_c^{min} above which dredge-up is triggered, (ii) the dredge-up efficiency (defined as $\lambda = \Delta M_{dredge} / \Delta M_c$, where ΔM_{dredge} and ΔM_c are, respectively, the amount of mass dredged-up to the envelope after a pulse and the increase in core mass during the time be-

tween two successive TPs), and (iii) the element abundances in the inter-shell material. The theoretical values of the dredge-up parameters are uncertain. Standard numerical models predict low dredge-up efficiencies (Boothroyd & Sackmann 1988), while models assuming diffusive overshooting predict highly efficient dredge-up events (Herwig et al. 1998). Actually both parameters λ and M_c^{min} affect the lifetime of the carbon-rich phase and the age interval for which carbon stars are present in a stellar population. Both parameters are also expected to depend on properties such as the stellar metallicity or its instantaneous mass and structure, but the available information on these relations is neither complete nor easy to extrapolate (e.g. Herwig 2000, Marigo et al. 1999). Our models assume constant λ and M_c^{min} . With this assumption, reproducing the luminosity function of carbon stars in the LMC requires intermediate dredge-up efficiencies and leads us to adopt $\lambda = 0.75$ and $M_c = 0.58$ (Groenewegen & de Jong 1993, Marigo et al. 1996). The chemical composition of the dredged-up material is taken from Boothroyd & Sackmann 1988.

The hot bottom burning (HBB, also known as envelope burning) is the second process affecting the chemical evolution of TP-AGB stars. This process is responsible for the destruction of newly dredged-up material at the base of the stellar envelope, in particular of carbon, and it thus prevents the formation of carbon rich stars in certain cases (Boothroyd et al. 1995). Envelope burning invalidates core mass-luminosity relations that were considered standard in the early 1990s (Blöcker & Schönberner 1991), and allows growth to higher luminosity (see Marigo et al. 1999b for a review). This triggers high mass loss rates, which in turn reduces the total lifetime of the TP-AGB phase and the final core mass. The semi-analytical treatment of hot bottom burning requires to set the critical envelope mass necessary for ignition at the basis of the envelope. We have used the condition derived by Wagenhuber & Groenewegen (1998). Combined with the mass loss prescription described below, this ensures agreement with empirical initial-final mass relations and with the age dependence of the TP-AGB contributions to the light of star clusters (Mouhcine & Lançon 2002).

We have used the highly detailed analytical representations of Wagenhuber & Groenewegen (1998) for both the core mass/luminosity, and core mass/interpulse period relations. Both third dredge-up and envelope burning were taken into account to calculate the evolution of the chemical abundance of stellar envelopes through the TP-AGB phase.

3.2.2 Mass loss

Mass loss along the TP-AGB is represented by the prescription of Blöcker's (1995), which was derived from the hydrodynamical models of Long Period Variable stars of Bowen (1988):

$$\dot{M} = 4.83 \cdot 10^{-9} \eta L^{2.7} M^{-2.1} \dot{M}_R \quad (1)$$

η is the mass loss efficiency, and \dot{M}_R is Reimers's standard mass loss rate (i.e., $\dot{M}_R = 1.27 \cdot 10^{-5} M^{-1} L^{1.5} T_{eff}^{-2}$). This formulation reflects the strong increase of the mass loss at the end of the AGB evolution, the so-called superwind phase. The mass loss efficiency used is $\eta = 0.1$, again as a result of calibration against carbon star populations of the LMC (Groenewegen & de Jong 1994). η is expected to depend on metallicity through variations in the gas-to-dust ratio and in the resulting radiative acceleration, but also through the essentially unknown metallicity dependence of the LPV pulsation properties. In the absence of reliable relations, we keep η constant, and thus include no explicit metallicity dependence in the mass loss rate. The metallicity dependence appears

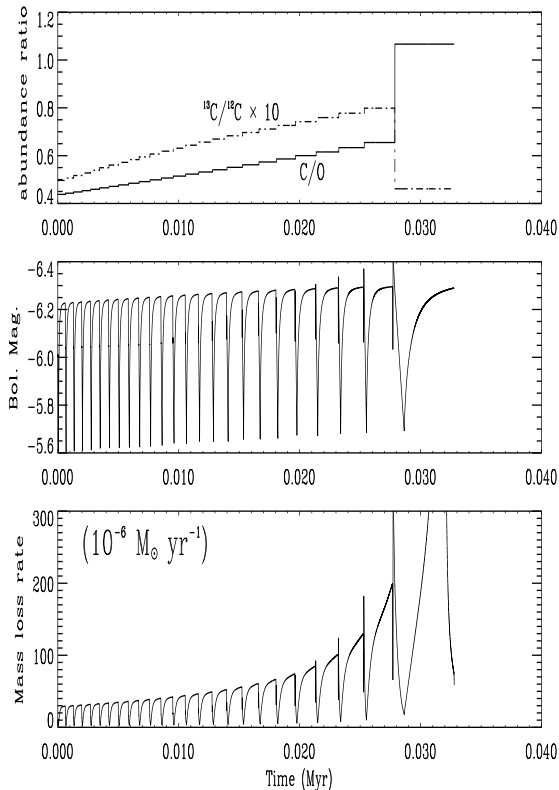


Figure 2. AGB evolution of the $4 M_{\odot}$ model with $Z=0.0004$. The top frame shows the $^{13}\text{C}/^{12}\text{C}$ and C/O ratios, the middle frame gives M_{bol} , and the lower frame the mass loss rate.

only via the metallicity dependent location of giant stars in the HR diagram. Note that different mass loss prescription with appropriate mass loss efficiencies, within the framework of a self-consistent model of stellar populations, describe the stellar population properties equally (see also Groenewegen & de Jong 1994).

3.2.3 The formation of carbon stars

At present, there seem to be two leading processes to form carbon stars: the first invokes dredge-up of carbon to the envelope during the AGB phase (Iben & Renzini 1983), and the second involves binary mass transfer of carbon from a once more massive but now degenerate companion (Jorissen & Mayor 1992). Carbon stars formed via the second channel fall below the red giant branch tip in the HR diagram. Those stars are observed without the radioactive s-process element technetium that specifically identifies stars on the TP-AGB (van Eck & Jorissen 1999). They can be separated statistically from the intrinsic technetium-rich stars, as the latter are on average cooler and brighter. Rebeirot et al. (1995) have surveyed the SMC for carbon stars. They found that faint carbon stars ($M_{\text{bol}} \leq -3.2$) contribute less than a few percent, by number, to the total number of carbon stars (e.g. 4-5%). In the rest of the paper carbon stars formed via binarity channel will not be counted. We consider only carbon stars formed via the third dredge-up channel. The formation of the evolution of carbon stars are investigated using the model described in the previous subsections.

In Fig. 1 we present the magnitudes at which stars with different initial masses leave the E-AGB phase and enter into the TP-

AGB phase, magnitudes at which they become carbon stars, and finally magnitudes at which they leave the AGB phase and become Post-AGB stars (see also Iben 1981, Marigo et al. 1999). For each metallicity of the grid, the evolutionary tracks associate stellar ages with the transition magnitudes. As expected with the adopted mass loss prescription, the bolometric magnitude reached at the end of the TP-AGB phase depends on the metallicity as well as on the initial mass of the star; the lower the metallicity, the brighter the termination magnitude of the TP-AGB. In addition, the lower the metallicity, the larger is the fraction of the TP-AGB lifetime spent as a carbon star; the evolution of this fraction as a function of the initial stellar mass peaks around $2 - 2.5 M_{\odot}$ independently of the initial metallicity. This mass range appears to be the privileged mass range for the formation of carbon stars at all metallicities (see Mouhcine & Lançon 2002 for more information).

Fig. 2 shows the evolution of bolometric magnitude, mass loss rate, C/O and $^{13}\text{C}/^{12}\text{C}$ of a $[4 M_{\odot}, Z=Z_{\odot}/50]$ model. The effect of HBB is clear: as the evolution proceeds, each dredge-up event brings about an increase of the C/O ratio (with $\text{C}/\text{O} = [n(^{13}\text{C}) + n(^{12}\text{C})] / [n(^{16}\text{O}) + n(^{17}\text{O})]$, ^{18}O has a very small contribution). But as long as the envelope mass is high enough to maintain a hot temperature at the base of the envelope, the CNO cycle transforms dredged-up ^{12}C into ^{13}C and ^{14}N . This increases the $^{13}\text{C}/^{12}\text{C}$ ratio and keeps the C/O ratio below unity. At the last thermal pulse, hot bottom burning has ceased because the large mass loss rate has dramatically reduced the mass of the envelope. The C/O ratio climbs abruptly. The model passes through $\text{C}/\text{O}=1$ and continues up to ~ 1.1 at the time when the star ends the TP-AGB phase, reaching a bolometric magnitude of $M_{\text{bol}} = -6.3$.

From the initial mass-bolometric magnitude diagrams of Fig. 1, one can already deduce very interesting features concerning the evolution of populations of intermediate mass stars. The youngest AGB populations, observed in stellar populations with main sequence turn-off masses $M_{\text{TO}} \sim 5 M_{\odot}$, will be oxygen rich. As time goes by and the turn-off mass decreases, carbon stars will occupy increasing fractions of the TP-AGB, both in terms of their luminosity range in the HR diagram and in terms of numbers. A maximum is reached for $M_{\text{TO}} = 2 - 2.5 M_{\odot}$. The fraction of the TP-AGB lifetime a star spends as a carbon rich object is largest for these initial masses (Mouhcine & Lançon 2002). Subsequently, when the turn-off mass further decreases, this fraction shrinks and the relative numbers of carbon stars drops.

The diagrams of Fig. 1 display a strong sensitivity to metallicity. For the same initial mass, the fraction of the TP-AGB lifetime spent as a carbon star increases when the metallicity decreases. The following processes contribute to this result: (i) less dredge-up of carbon rich material from the core is needed to reach $\text{C}/\text{O} \geq 1$ in metal-poor stars; (ii) at lower metallicities, the core mass at the beginning of the TP-AGB phase is larger, leading to earlier third dredge-up events; and (iii) the interpulse period is longer at lower metallicities, leading to more violent dredge-up events (see WG98 for more details); the He-shell accretes material for a longer time, and therefore more carbon-rich material is dredged-up to the envelope at each thermal pulse, while the envelope mass does not change significantly in comparison to the case where the metallicity effect on the interpulse period is neglected.

3.3 Chemical Evolution

While star clusters may be represented with SSP models, the Local Group galaxies had more continuous SF histories. A self-consistent modeling of the carbon star populations of such systems must be

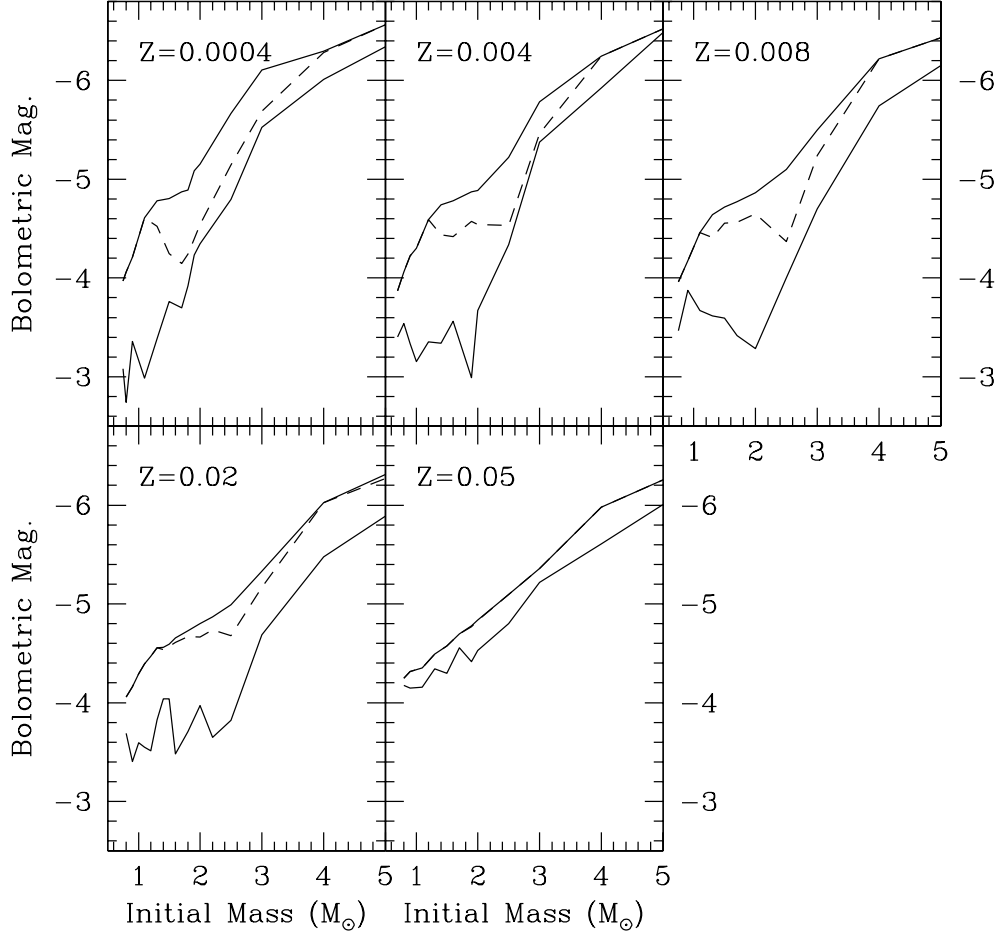


Figure 1. Bolometric magnitudes versus initial mass for three characteristic stages of the AGB phase, namely the start of the TP-AGB (bottom line), the transition between the oxygen-rich phase and the carbon-rich phase (dashed line), and the termination of the AGB phase. The predictions are those of our standard stellar model adopted in this work ($\alpha = 2$, $\eta = 0.1$ with Blöcker’s mass loss prescription). The initial masses are in solar units, the initial metallicity, Z , is indicated on each panel.

able to account for chemical evolution and for the resulting coexistence of stellar generations with different initial metallicities and ages. Carbon stars are present and dominate AGB stellar populations over an age range of a few Gyr, during which the chemical evolution may be efficient. In this subsection, we will present the chemical evolution model used in this work.

The formation of stars, the re-ejection of gas, and the evolution of the gas mass evolve according to Tinsley’s standard equation (1980) reducing the model to a set of few parameters that govern the evolution. The total gas mass evolves according to:

$$\frac{dM_{gas}}{dt} = -\psi(t) + R(t) + f(t) \quad (2)$$

where $\psi(t)$ is the star formation rate (SFR) and $R(t)$ is the gas return rate to the interstellar medium. $R(t)$ takes into account the finite lifetime of the turn-off stars, as derived from the stellar tracks also used to produce the synthetic stellar populations. We assumed instantaneous mixing of the ejected gas as well as instantaneous cooling of the hot gas component. The term $f(t)$ is an additional

gas accretion rate from the intergalactic medium. An exponentially decreasing infall rate is assumed (Lacey & Fall 1985):

$$f(t) = M_{tot} \frac{\exp*(-t/\tau_f)}{\tau_f} \quad (3)$$

where M_{tot} is the total mass at 20 Gyr and $\tau_f = 5$ Gyr is the accretion timescale for the formation of the galaxy. We assume that the accreted gas has primordial abundances (Walker et al. 1991). No outflow is considered in the models.

The evolution of the abundance X_i of element i in the interstellar medium obeys:

$$\frac{dX_i M_{gas}}{dt} = -X_i \psi(t) + R_{i,1}(t) + f_{SNIa} R_{i,2}(t) + (1 - f_{SNIa}) R_{i,3}(t) + R_{i,4}(t) + X_{i,p} f(t) \quad (4)$$

Here, $X_{i,p}$ is the abundance in the infalling gas, which is taken to be primordial. $R_{i,1}(t)$ and $R_{i,2}(t)$ are described by the following equations:

$$R_{i,1}(t) = \int_{M_{low}}^{M_{Bmin}} \psi(t - \tau(m)) \phi(m) mp_i(m) dm \quad (5)$$

and

$$R_{i,2}(t) = \int_{M_{Bmin}}^{M_{Bmax}} \phi(m) \left[\int_{\mu_{min}}^{1/2} f(\mu) \psi(t - \tau(m)) d\mu \right] mp_i(m) dm \quad (6)$$

$mp_i(m)$ is the stellar yield of the chemical element i ejected by star of initial mass m , and $\phi(m)$ is the initial mass function (hereafter IMF). In the rest of the paper we adopt a power law IMF between the lower and upper cutoff masses $M_{low} = 0.8 M_{\odot}$ and $M_{up} = 120 M_{\odot}$ ($\phi(m) \propto m^{-\alpha}$, $\alpha = 2.35$).

$R_{i,2}(t)$ describes the enrichment from Type Ia supernovae (SNe Ia). These SNe Ia are assumed to originate in binary systems in which at least one of the stars is a white dwarf. The infall of gas from the companion pushes the mass above the Chandrasekhar limit, triggering a deflagration with subsequent disruption of the star. SNe Ia should be considered since they contribute a large fraction of iron. M_{Bmin} and M_{Bmax} are the lower and upper total masses of the relevant binary systems. We assume that the total mass of these binaries follows the same IMF as single stars. The initial mass range of the SNe Ia progenitors is taken from Greggio & Renzini (1983). $f(\mu)$ is the distribution function of binary system mass ratios, defined as the ratio between the secondary mass and the total mass m of the system. $R_{i,1}(t)$, $R_{i,3}(t)$ and $R_{i,4}(t)$ describe, respectively, the enrichment due to single stars with initial masses in different regions of the mass spectrum: $R_{i,1}(t)$ for stars with $M_{init} \leq M_{Bmin}$, $R_{i,3}(t)$ for stars with $M_{init} \in [M_{Bmin}, M_{Bmax}]$, and $R_{i,4}(t)$ for stars with $M_{init} \geq M_{Bmax}$. f_{SNIa} is the fraction of stars assumed to be in binary systems close enough to finally lead to SNe Ia events. A value of $f_{SNIa} \approx 0.1$, used in our calculations, has been derived from the observed SNe I and II rates in our Galaxy (Evans et al. 1989).

The most important inputs into a chemical evolution calculation are the stellar yields. Three different sources of chemical elements must be considered: the first are the massive stars ($M > 8 - 10 M_{\odot}$) which evolve into Type II supernovae, the second are the intermediate mass stars ($0.8 M_{\odot} < M < 6 M_{\odot}$) which evolve into planetary nebulae, and the third are the intermediate mass stars in close binary systems which become Type Ia supernovae.

For massive stars, we use the recent metallicity dependent stellar yields published by Portinari et al. (1998). They are based on the evolutionary tracks of the Padova group, and take into account both the material ejected by stellar winds and the explosive nucleosynthesis in SNe of Woosley & Weaver (1995). For intermediate mass stars, we use the synthetic evolution model discussed above to derive new metallicity dependent stellar yields (Mouhcine, in preparation). The yields for SNe Ia are taken from the improved $Z = Z_{\odot}$ W7 model presented in Thielemann et al. (1993). The mass of iron ^{56}Fe ejected is $0.63 M_{\odot}$, with no remnant. This yield is assumed to be metallicity-independent, which is a reasonable assumption based upon the similarity of Thielemann et al.'s $Z = Z_{\odot}$ and $Z = 0$ models.

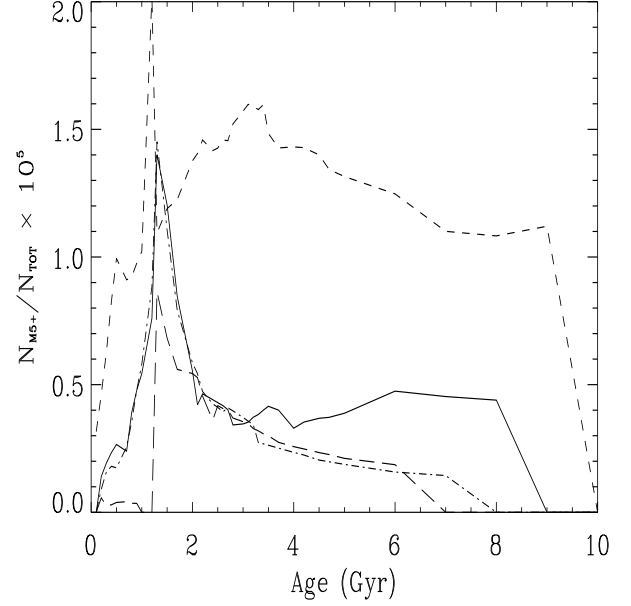


Figure 3. Evolution of the fraction of late-type M stars as a function of age for single stellar population for $Z=0.02$ (dashed line), $Z=0.008$ (solid line), $Z=0.004$ (long-dashed line), and $Z=0.0004$ (dot-dashed line). The effect of the metallicity on the late-type M star efficiency is obvious; the lower the metallicity, the harder is the formation of late-type M stars, and the lower is their contribution to the total star number.

4 STATISTICS OF AGB STARS IN A SINGLE STELLAR POPULATION

In this section we discuss the model predictions regarding the statistics of intermediate mass stars in SSPs. The formation and the evolution of AGB stars is investigated using the model described in the previous section.

The observational techniques used to recognize AGB stars from other late type stars in external galaxies, and to classify them as oxygen-rich or carbon-rich, are based on colour criteria. We define carbon stars as stars evolving along the TP-AGB phase with $C/O > 1$. The narrow band filter system mentioned in Sect. 1 allows an empirical separation that agrees with this definition. The formal definition of the late type oxygen-rich stars requires special understanding.

For comparison with the data summarized in Section 2, our predictions regarding late type M stars must comply with the selection criteria currently applied by observers rather than correspond with a more theoretical definition of oxygen-rich TP-AGB stars. When only photometric data exists, stars with spectral type equal to M5 or later (M5+ hereafter), can in principle be defined as oxygen-rich stars redder (cooler) than a given colour (effective temperature), assuming a correspondence between colour (effective temperature) and spectral type. Richer et al. (1985) and Pritchett et al. (1987) defined M5+ stars as stars with $V-I > 2$. Albert et al. (2000) adopted $R-I > 0.9$ as selection criterion. Measurements on solar neighborhood spectra show a good correspondance between these two criteria (see Fig. 1 of Lançon & Mouhcine, 2002). We have to mention that those colour criteria are based on the earlier observations of LMC M stars of Blanco et al. (1980). In order to be able to compare our predictions with the observational findings, we

adopt a colour criterion similarly to the observational procedures. We thus define “M5+ stars” as oxygen rich stars with $V-I > 2$, independently of the stellar population metallicity (Richer et al. 1985), and with an initial mass in the range of the mass spectrum bound to evolve through the AGB evolutionary phase. To project this colour criterion into the theoretical HR diagram, we use the metallicity dependent colour-effective temperature relation of Bessell et al. (1989).

For a single burst population of age t and of total mass M_{TOT} , the total number of stars is

$$N_{SSP}(t) = M_{TOT} \int_0^{M(t)} \frac{\Phi(m)}{m} dm, \quad (7)$$

where $M(t)$ is the initial mass of the stars with lifetime t . At an age t , stars of initial mass $M_{init} = M_{TO}(t)$ leave the main sequence (MS), while stars with $M_{init} = M_{TO}(t - T_i) > M_{TO}(t)$ leave the post-MS evolutionary phase i . The number of stars between the main sequence and the end of phase i is:

$$N_i = M_{TOT} \int_{M_{TO}(t)}^{M_{TO}(t-T_i)} \frac{\Phi(m)}{m} dm \quad (8)$$

Using the approximations that: (i) in a SSP the post-main sequence stars occupy a very limited interval of initial masses, (ii) the typical lifetimes of different post-main sequence phases are very short in comparison with the MS lifetime of the turn-off mass, we can write (see e.g. Renzini & Buzzoni 1986, Girardi & Bertelli 1998):

$$N_i \approx M_{TOT} b(t) T_i \quad (9)$$

where $b(t) = \phi[M_{TO}(t)]/M_{TO}(t) |dt/dM|^{-1}$ is the post-main sequence star production rate, and T_i is the lifetime of a turn-off star between the turn-off and the end of phase i . Even though this calculation involves simplistic approximations, it provides us with a tool for a qualitative understanding of the evolution of the N_C/N_{M5+} ratio, since it can be used to relate the number ratio directly to the ratio of the durations of the carbon-rich phase (T_c) and the late M-type phase (T_{M5+}).

$$\frac{N_C}{N_{M5+}}(t) \approx \left[\frac{T_c}{T_{M5+}} \right]_{M_{TO}(t)} \quad (10)$$

In Figure 3 we show the time evolution of the fractional number of M5+ stars among all stars, N_{M5+}/N_{TOT} , in stellar populations with metallicities between $Z/Z_\odot = 1/50$ and $Z/Z_\odot = 1$. The models evolve from an instantaneous burst with a Salpeter IMF. To compute N_{TOT} we consider only stars that contribute to the population light budget (i.e. the stellar remnants are not considered). The models evolve from an instantaneous burst with the Salpeter IMF specified in Sect. 3.3. We predict a rapid increase of the fraction of M5+ stars with time, with a maximum at about 1 Gyr because the duration of the TP-AGB reaches a maximum for stars with these lifetimes. After the maximum, the number fraction of M5+ stars evolves and decreases slowly. It goes to zero when the coolest temperature on the isochrone is higher than that of an M5+ star. The striking features shown in Fig. 3 are that the maximum N_{M5+}/N_{TOT} ratio and the range of ages over which M5+ stars are numerous decrease rapidly with metallicity.

Figure 4 displays the evolution of N_C/N_{M5+} , for solar and LMC metallicities. As expected from Fig. 1, carbon stars are predominant at low metallicities. In addition, at a given metallicity, the distribution of N_C/N_{M5+} evolves with time. The ratio rises rapidly up to a maximum just before 1 Gyr of age, and decreases for older systems. This temporal evolution of N_C/N_{M5+} is directly related

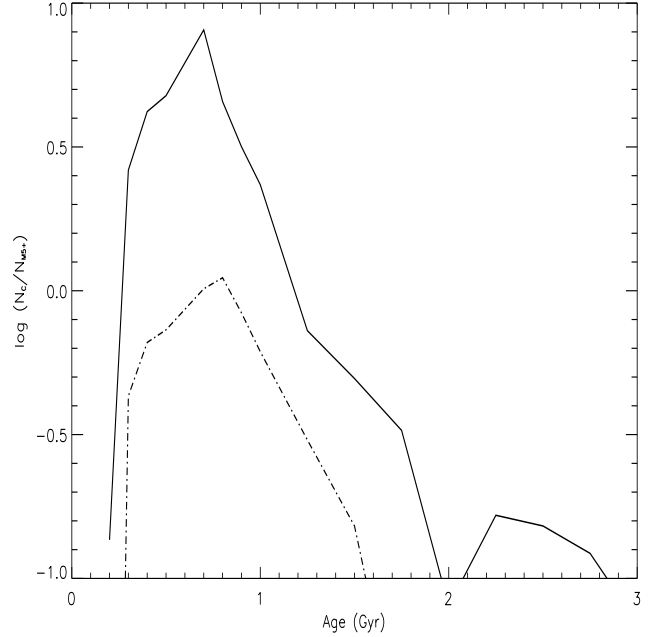


Figure 4. Temporal evolution of the carbon stars to M5+ stars ratio vs. metallicity for instantaneous burst scenario for $Z=0.008$ (continuous line) and $Z=0.02$ (dotted-dashed line). The effect of the initial stellar population abundances is clear; the lower the metallicity, the higher is the ratio.

to changes in the duration of the carbon rich phase, T_c , relative to the total lifetime in the TP-AGB phase, T_{TP-AGB} , as the turn-off mass of the stellar population decreases. This relative duration is largest for stars with initial masses in the range of $2 - 2.5 M_\odot$, which have a main sequence lifetime close to 1 Gyr.

In summary, metallicity has two main consequences on the populations of late-type stars. The number proportion of M5+ stars decreases intrinsically with metallicity because the giant branch becomes bluer with decreasing metallicity. At a given age after a star-burst, N_C/N_{M5+} is a strong function of metallicity. One relatively metallicity-independent property is that the maximum N_C/N_{M5+} occurs when the turn-off mass is of $2 - 2.5 M_\odot$, because stars with these initial masses have the longest carbon rich phase independently of the stellar metallicity.

As a step towards the study of the complex stellar populations of galaxies, we briefly look at the late type stars of models with a constant SFR and a fixed metallicity. The proportion of M5+ stars is given by the averages of the curves in Fig. 3 over the accumulated range of ages. The fractional number of M5+ stars increases over the first 1–2 Gyr, then stabilises for many billions of years. It is reduced progressively only at very old ages. As a result of the larger contrast in Fig. 4 (note the logarithmic scale), N_C/N_{M5+} keeps a strong dependence on time even when the SFR is constant. Because N_C/N_{M5+} rises extremely rapidly, stars of the first generation will dominate the number of carbon stars during the first Gyr of evolution. The population of carbon stars is essentially stationary after the first $\sim 1 - 1.5$ Gyr. Carbon stars with lower initial masses that remain to be born represent only a tiny fraction of the carbon stars that already appear and die in a stationary fashion. As a result, N_C/N_{M5+} slowly decreases by dilution after the first few billions of years. The maximal and the quasi-stationary values reached by N_C/N_{M5+} both increase with decreasing Z . It is interesting to men-

tion that the difference between the quasi-stationary N_C/N_{M5+} of a constantly star forming galaxy model and the maximum N_C/N_{M5+} reached after a burst is larger at lower metallicities. Indeed, in metal poor environments the range of initial masses capable of producing carbon stars is broader than at high Z ; the carbon star episode following a burst is more stretched in time, and the contrast with a constant star formation situation is less pronounced.

5 EFFECTS OF MASS LOSS ON CARBON STAR STATISTICS.

The majority of observational techniques applied to search for carbon stars operate in the optical. Those techniques are biased towards unobscured carbon stars and may be missing the majority of mass loosing stars. The transition from optically visible stars to purely infrared sources is related to the mass-loss which produces the circumstellar envelopes. It is important for our purpose to know when this transition occurs, and how much time a TP-AGB star spends as a dust-obscured object. In this section we derive an estimate of the number fraction of carbon stars that may be missed in optical surveys.

To estimate the lifetime fraction that a carbon star spends as optically invisible, we assume that the stars is no longer observable when the optical depth at $1\mu\text{m}$, $\tau_{1\mu\text{m}}$, is higher than a given critical value ($\tau_{1\mu\text{m}} \gtrsim \tau_{\text{crit}}$). To estimate the optical depth we have to construct dusty envelope models around late type AGB stars. To do so we assume (i) spherical symmetry, (ii) constant mass outflow and expansion velocity. Neglecting the inverse of the circumstellar shell outer radius with respect to the inverse of the grain condensation radius, which is not bad approximation as we restrict ourselves to the near-infrared (Rowan-Robinson 1986), the optical depth as a function of wavelength is given by:

$$\tau_\lambda \propto \frac{\dot{M} \Psi}{R_c v_d} \frac{Q_{\text{ext}}(\lambda, a)/a}{\rho_{gr}(a)} \quad (11)$$

where $Q_{\text{ext}}(\lambda)$ is the sum of the absorption and scattering coefficients of the dust, a the grain radius, ρ_{gr} the grain density, R_c the inner radius of the dust shell, called also the dust condensation radius, v_d the dust outflow velocity, and Ψ the dust-to-gas ratio. The condensation radius is taken to vary as $R_c \propto [T_{\text{eff}}/T_c]^{(4+\beta)/2}$ where the parameter β gives the overall wavelength dependence of the grain properties, $Q(\lambda) \propto \lambda^{-\beta}$ (Jura 1983, Bedijn 1987), and equals ~ 1 for amorphous carbon dust. Grain properties at $1\mu\text{m}$ are taken from Suh (2000) for $a = 0.1\mu\text{m}$ grains, with a grain density of $\rho_{gr} \sim 2.5 \text{ gr cm}^{-3}$. The condensation temperature of amorphous carbon grains is taken to be $T_c = 1000 \text{ K}$ (Le Sidaner & Le Bertre 1996). The dependence of both Ψ and v_d on the fundamental stellar parameters are taken from Habing et al. (1994) and Vassiliadis & Wood (1993).

Figure 5 shows the evolution of the fraction of its carbon-rich lifetime that a star spends as an optically invisible object, as a function of initial mass for $Z=0.02$ and $Z=0.008$. Two different choices of the critical optical depth ($\tau_{\text{crit}} = 1, 3$) are shown. This range of optical depths was chosen to reflect the uncertainties on different ingredients used to construct the envelope models, known in order of 1-3 (Jura, private communication).

The most striking feature, from the population synthesis point of view, that is coming out from this plot is the dip at initial masses of $\sim 2.5 M_\odot$. One has to keep in mind that those stars form the bulk of the carbon stars as shown in Sec. 4. These stars remain optically visible for most of their carbon rich phase. Their fundamental

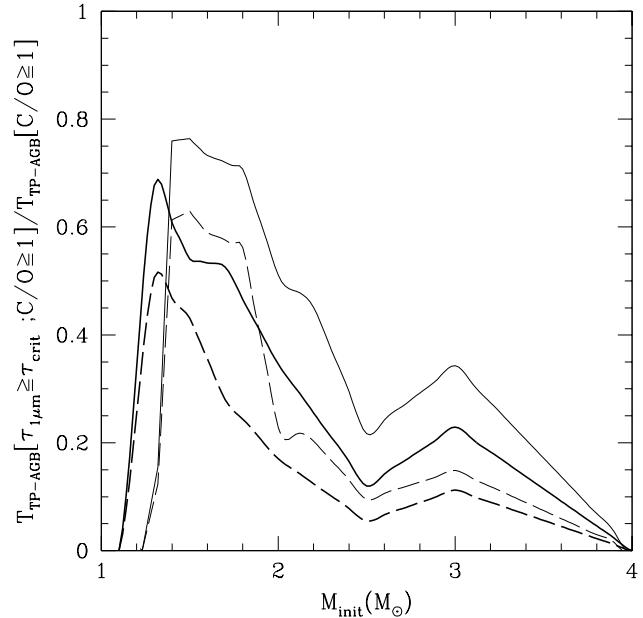


Figure 5. Fraction of the total carbon rich lifetime spent as an optically invisible infrared source, as a function of initial mass, for $Z=0.02$ (thin lines) and $Z=0.008$ (thick lines) metallicities. Stars are assumed to be no longer optically visible when the optical depth at $1\mu\text{m}$ is larger than the unity (continuous lines) or than 3 (dashed lines). The plot shows that higher the star metallicity, larger is the fraction of carbon-rich phase spent as being optically invisible. See text for more details.

parameters are such that they trigger a superwind only very late in their evolutionary history. This is in agreement with the observational finding that the majority of carbon stars have low mass loss rates. The plot shows also that decreasing initial stellar metallicity decreases the lifetime fraction that a carbon star spend being optically invisible, reflecting the extreme sensitivity of the optical depth to metallicity. This is of great importance for our purpose as carbon stars as found preferentially in metal-poor systems, and that the galaxy sample for which carbon star statistics are available in the literature is composed mainly by metal-poor galaxies.

As a consequence, the numerical values in Fig. 5 at the smallest and largest initial masses are very sensitive to choices that enter our definition of the transition from optically visible to obscured stars or from oxygen-rich to carbon-rich stars. In comparison, the results for intermediate initial masses are robust, because all relevant evolutionary phases are of longer duration.

Using Eq. 9, one should expect that, for a single stellar population, the number fraction of optically invisible carbon stars among all carbon stars will behave as the ratio of the lifetimes in the corresponding phases as shown in Fig. 5 ($N_{\text{CIR}}/N_C \approx [T_{\text{CIR}}/T_C]_{M_{\text{TO}}}$, where M_{TO} is the current turn-off mass). Hence when the stellar population evolves, the fraction of dust-surrounded carbon stars decreases with a minimum at $\sim 1 \text{ Gyr}$, when $M_{\text{TO}} \sim 2.5 M_\odot$. For older stellar populations, the fraction of obscured carbon stars is expected to increase while, as discussed already, the whole population of carbon stars shrinks in importance.

We conclude that the contribution of obscured carbon stars to the total number of carbon stars is relatively small (10-20 % at $\sim 1 \text{ Gyr}$) and that the global statistics of carbon stars will not be affected dramatically if one uses only the carbon stars found in op-

tical surveys. In the rest of the paper we will calculate the evolution of the total number of carbon stars including optically visible and invisible sources.

6 STATISTICS OF AGB STARS IN COMPLEX STELLAR POPULATIONS.

Using the results of the previous sections, it is possible to give theoretical predictions for the evolution of various late-type stellar populations for stellar systems with complex SF histories.

The number of carbon stars and late type M stars for a stellar population with a star formation rate $\psi(t)$ is given by:

$$N_C(t) = \iint \psi(t - \tau(m)) \frac{\phi_{AGB}(m)}{m} \epsilon_C(m, \tau, Z) dm d\tau \quad (12)$$

$$N_M(t) = \iint \psi(t - \tau(m)) \frac{\phi_{AGB}(m)}{m} \epsilon_M(m, \tau, Z) dm d\tau \quad (13)$$

where $\phi_{AGB}(M)$ is the IMF restricted to the mass range of stars that indeed evolve through an AGB phase. The adopted lower and higher initial masses of AGB progenitors depend slightly on the metallicity. $\epsilon_C(m, t, Z)$ and $\epsilon_M(m, t, Z)$ are derived from the evolution of the C/O abundance ratio in AGB star envelopes. $\epsilon_C(m, t, Z)$ describes, for a given initial mass and initial metallicity, when and for how long a TP-AGB star is carbon rich. $\epsilon_C(m, t, Z)$ is given by:

$$\epsilon_C(m, t, Z) = \begin{cases} 1 & \text{if } t \geq f_C(m, Z)T(m, Z) \\ 0 & \text{if } t < f_C(m, Z)T(m, Z) \end{cases} \quad (14)$$

$T(m, Z)$ is the time that elapses between the moment a star of initial mass m becomes an M5+ object and the moment it leaves the TP-AGB; $f_C(m, Z)$ is the fraction of this time the star spends as a carbon star. Similarly, $\epsilon_M(m, t, Z) = 1 - \epsilon_C(m, t, Z)$ indicates which stars are to be counted as M5+ objects.

As mentioned in Sect. 3.3, we restrict ourselves to one-zone galaxy models, assume ideal mixing, and start the chemical evolution from a homogeneous gas cloud of primordial composition. The global SFR is assumed to be a function of the total gas content (Schmidt 1963), with the star formation efficiency as a free parameter. The efficiency is chosen such as to mimic the SF histories along the Hubble sequence, as the spectrophotometric properties of this galaxy sequence is primarily dictated by the characteristic time scale for the star formation (e.g. Sandage 1986, Charlot & Bruzual 1991, Fritze von Alvensleben & Gerhard 1994, Fioc & Rocca-Volmerange 1997).

$$\psi(t) = \frac{\rho_g^k(t)}{\tau_*} \quad (15)$$

where τ_* is the star formation timescale and ρ_g the available gas mass. We will use the timescales of Fioc & Rocca-Volmerange (1997) here. As the Local Group galaxies are mostly dwarfs (irregulars or spheroidals) or late-type galaxies, we will restrict our calculations to timescales typical of Sa-type to Irr-type galaxies. As we are interested in the systematic behavior of carbon star statistics and are not focusing on any particular stellar system, we do not consider other forms of SFRs (bursting star formation for example).

Figure 6 shows the age-metallicity relation for the closed box galaxy models of this paper, with Schmidt's exponent k equal to unity. The metallicity rises rapidly at early times. The rate of rise in $[\text{Fe}/\text{H}]$ is largest when the SF timescale is short, i.e. with the

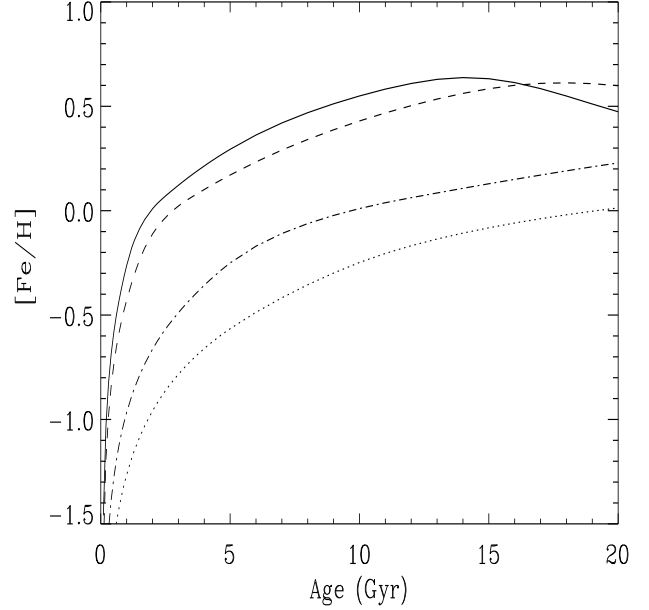


Figure 6. Age-metallicity relation for the different star formation histories discussed in this paper, assuming closed box galaxy models. $[\text{Fe}/\text{H}]$ refers to the interstellar matter. Different lines refer to galaxies with different SF timescales τ_* . The solid line represents Hubble type Sa, the dashed line type Sb, the dot-dashed line type Sc and dotted line Irregular galaxies. The longer the SF timescale, the slower the chemical evolution (see text).

SF scenarios appropriate for early type spiral galaxies. These models also have the largest initial star formation efficiency, and they are the first to reach their maximum star formation rate. The AMRs flatten for older systems, mainly due to decreasing star formation rates. When star formation has been negligible for a long enough period of time, $[\text{Fe}/\text{H}]$ may decrease as a result of the dilution of interstellar iron in iron-poor low mass star ejecta (the iron abundance is significantly determined by the contribution of SNe Ia). The chemical evolution in models with gas infall (Eq. 3) is qualitatively similar, except that it is slower because the accreted gas is assumed to be metal-free.

Figure 7 shows the evolution of N_C/N_{M5+} and of the relative number of carbon stars in the whole stellar population for the SF histories considered above, for both closed box and infall models, and $k = 1$. The generic behavior of N_C/N_{M5+} as a function of age can be understood as follows, in the light of the discussion in Sect. 4. Regardless of the details of the star formation history process (i.e. the SF timescale) or the galaxy formation (closed box or infall model), the ratio sharply increases and reaches its maximum at an age of ~ 1 Gyr. When the massive carbon stars of the first generation of stars die, two types of carbon stars replace them. A second generation of carbon stars with the same high initial mass and a slightly higher metallicity appears, but also carbon stars with lower initial mass appear for the first time. The latter have the same metallicity as the more massive carbon stars that are dying. A longer carbon rich phase is associated with their lower initial mass. The increase in the duration of the carbon rich phase is rapid compared to changes in the SFR. As a consequence, those lower mass carbon stars will dominate, by number, the whole carbon star population. The relative number of carbon stars continues to increase until stars with the longest carbon rich phase (i.e. initial masses of $2.5\text{--}2\text{ M}_\odot$

and main sequence lifetimes of the order of 1 Gyr; see Fig 1) evolve off the main sequence. Then, a quasi-stationary carbon star population is established: the birth and death rates of the predominant carbon stars are balanced. Changes in the carbon star proportions then essentially reflect the evolution of the metallicity, with a delay of the order of 1 Gyr which is short compared to the evolutionary timescale of the SFR. N_C/N_{M5+} decreases, tracing the metallicity increase with increasing age and with decreasing star formation timescale.

It is noteworthy that the maximum reached by the N_C/N_{TOT} ratio increases with decreasing star formation timescale. Indeed, the carbon stars of the first generations are compared to a total number of stars that will be smaller if star formation decreases rapidly. In contrast, the maximum reached by the N_C/N_{M5+} ratio decreases with decreasing SF timescales. This essentially reflects the evolution of metallicity, as the dominant carbon and M5+ stars are of similar age.

In summary, the figures show the predominance of carbon stars relative to late type M stars and the high carbon star formation efficiency for metal-poor systems corresponding to stellar systems with low star formation rate. Models calculated assuming gas infall present the same qualitative behavior but with scaled-up N_C/N_{M5+} and N_C/N_{TOT} ratios due to the slower chemical evolution.

In the following subsections, we will compare our number count models combining the evolutionary population synthesis models and the chemical evolution models with the observed properties described in Sec. 2.

6.1 The evolution of N_C/N_{M5+} as a function of metallicity

By combining the temporal evolution of N_C/N_{M5+} and of the metallicity, we can derive the evolution of N_C/N_{M5+} as function of $[Fe/H]$. Figures 8 and 9, respectively, show the resulting predictions in the case of closed box and infall models, with Schmidt's exponent $k = 1$. For direct comparison, the observational data for galaxies with good carbon star statistics are over-plotted on Fig. 8. N_C/N_{M5+} ratios are taken from Groenewegen (1999), apart for NGC 8266 taken from Letarte et al. (2002) and IC 1613 estimated from Albert et al (2000) data set. $[Fe/H]$ represents the best available estimate of the interstellar medium metallicity. Very good agreement is found. The predicted sequence in the N_C/N_{M5+} vs. $[Fe/H]$ plane exhibits the same trend as the observed one. Metal-poor stellar systems have a larger number of carbon stars relative to number of late type M stars. The theoretical curves delineate quite well the boundaries of the locus of the observational data points. To give the reader an idea about the time evolution effect on the considered diagram, some reference ages are indicated in Fig. 9.

For stellar populations younger than 0.8-1 Gyr, we observe a dramatic evolution of N_C/N_{M5+} as a function of metallicity. It must be kept in mind that the dominant carbon star populations in those systems have a narrow range of (low) stellar metallicities. The first generation of stars with initial mass in the privileged range of 2–2.5 M_\odot produces carbon stars after about 1 Gyr; carbon stars with these progenitor masses remain predominant. The star formation timescale determines how rapidly the interstellar medium is enriched at early times. For older stellar systems, carbon stars form at a quasi-stationary rate, and N_C/N_{M5+} essentially traces metallicity. Its quasi-monotonic evolution with metallicity is a natural consequence of the evolution of carbon star properties as a function of metallicity. The number ratio expresses the metallicity dependance of the ratio between the durations of the carbon rich phase and of the M5+ phase, weighted by the IMF. The models for

old populations form a well-defined sequence in the N_C/N_{M5+} vs. $[Fe/H]$ diagram. The locus of the models depends very little on the assumed SF history. The gas infall process has no major effects on this locus either. Considering infall will only slow down the chemical evolution of the stellar population, and consequently the stationary carbon star formation will take place at lower metallicity, with a higher N_C/N_{M5+} ratio as for the closed-box models. This is consistent with the observational result pointed out by Brewer et al. (1995), i.e. that the N_C/N_{M5+} ratio is determined by the local metallicity rather than by galactic morphological (or spectroscopic) type.

The evolution of the statistics of carbon star populations as a function of metallicity shows a very small sensitivity to the exponent of the star formation law, which affects the shape of the SFR. This is consistent with the result discussed above: the global properties of carbon star populations are determined mainly by metallicity rather than by the shape of the SF history.

In the rest of the paper we restrict ourselves to $k = 1$.

6.2 The mean carbon star luminosity as a function of metallicity

As discussed in Sect. 2, the second observed property of carbon star populations is their mean bolometric luminosity. We use the following definition:

$$\langle M_{Bol,C} \rangle = -2.5 \log \left(\frac{\sum_{i=1}^{N_C} L_{i,C}}{N_C} \right) + 4.74 \quad (16)$$

where $\sum_{i=1}^{N_C} L_{i,C}$ is the sum of the luminosity contributions of all carbon stars, and N_C is the total number of carbon stars.

Metallicity has a significant effect on the time evolution of the luminosity of the brightest TP-AGB stars of single stellar populations. Indeed, metallicity affects the mass loss rate, and hence the initial-final mass relation: the lower the metallicity, the lower is the mass loss rate, and the higher are the final core mass and bolometric luminosity (Mouhcine & Lançon 2002, Zijlstra 1998). At a given turn-off mass, the brightest carbon stars of a metal-rich SSP will be fainter than those of a metal-poor SSP.

Figure 10 shows the evolution of $\langle M_{Bol,C} \rangle$ with metallicity, for the star formation histories and galaxy formation scenarios considered in this paper. A few reference stellar population ages are indicated.

The evolution of $\langle M_{Bol,C} \rangle$ as a function of $[Fe/H]$ can be summarized as follows. For stellar populations younger than ~ 1 Gyr, carbon star populations become fainter as time evolves. As already pointed out, young systems are dominated by the first generation of chemically homogeneous carbon stars. As the turn-off mass of this first generation decreases, the final stellar core mass and hence the final luminosity of the predominant carbon stars decreases (Aaronsen & Mould 1980, Bressan et al. 1994, Mouhcine & Lançon, 2002). The shift between the rising curves for various star formation timescales is due to the differing rates of metal enrichment of the galaxy gas; the intermediate mass stars forming out of this enriched gas have not yet reached the carbon rich phase.

For stellar systems older than ~ 0.8 -1 Gyr, when carbon star formation has reached the quasi-stationary regime, the evolution of $\langle M_{Bol,C} \rangle$ is completely insensitive to metallicity. As the stellar populations grow older and more evolved chemically, (i) the carbon star sequence in the HR diagram becomes less extended which reduces the total luminosity of the carbon star population, (ii) the number of carbon stars decreases. As both the total luminosity and

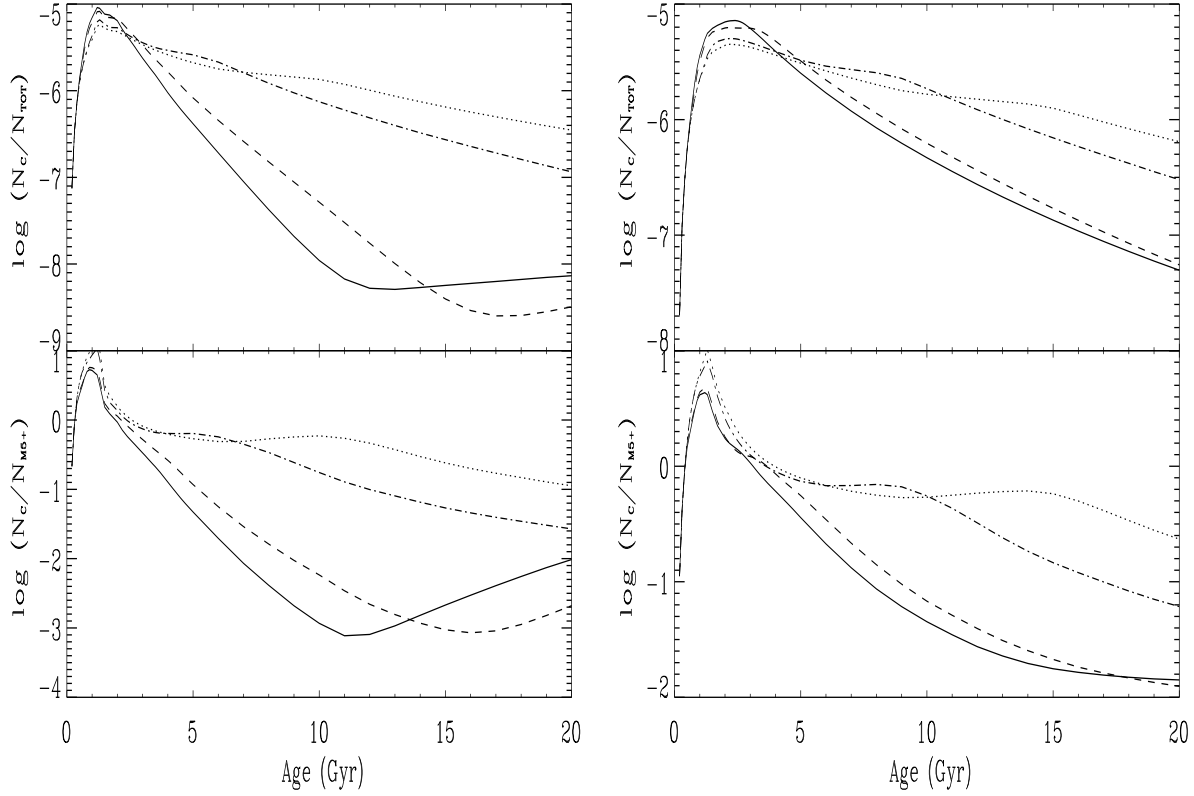


Figure 7. Left: Evolution of the logarithmic number ratio of carbon rich to late M stars (bottom plot), and of the logarithmic number fraction of carbon rich among all stars (top plot). The lower the metallicity, the higher is the carbon star contribution to the total number of stars. The chemical evolution is computed with the closed box assumption. Right: Similar to the left panel but assuming that the stellar populations are formed by gas infall (see text)

the total number of carbon stars scale with the metallicity, the ratio is relatively independent of it.

As in the case of N_C/N_{M5+} , the model adopted for the galaxy formation (infall or closed box) does not affect the evolution of $\langle M_{Bol,C} \rangle$ with galaxy metallicity dramatically, except that the chemical evolution for stellar systems formed via gas infall is slower. The “plateau” in $\langle M_{Bol,C} \rangle$ is thus reached at lower metallicity.

The predicted values of $\langle M_{Bol,C} \rangle$ for stellar systems with stationary carbon star formation lie between -4.6 and -4.7. Comparison with the observed values in Local Group galaxies with good carbon star statistics and good evidence that the observed carbon stars are indeed on the TP-AGB (e.g. galaxies that display an extended giant branch), shows very good agreement: as recalled in Sect. 2.2, observational values lie around -4.7.

This result leads some investigators to consider carbon star populations as potential distance indicators, better in some respects than the Cepheids for example (higher bolometric luminosity, single epoch of observation, reduced interstellar reddening with near-infrared observations, low contamination from dwarf field stars). Determinations of the distance modulus to M31 by Brewer et al. (1996) and Nowotny et al. (2001) using this technique are in good agreement with other distance determinations (Freedman & Madore 1990).

6.3 The normalized carbon star number as a function of metallicity

Combining the number count model and the chemically-consistent spectrophotometric model, we can predict the relation between metallicity and the number of carbon stars normalized to the total stellar luminosity. This relation is important in the sense that it enables us to distinguish between the two competing explanations for the correlation between N_C/N_{M5+} and metallicity (see Sect. 2.1).

Figure 11 shows the evolution of the carbon star number normalized to the V-band luminosity of the parent galaxy, as a function of metallicity, for our standard evolutionary scenarios. The evolution of the carbon star number normalized to the B-band light is similar, they are obtained from the previous ones by a shift of 0.4 (B-V), which remains small at all times.

Again, the evolution of the normalized number of carbon stars as function of metallicity can be split up into two regimes. For stellar populations younger than about 1 Gyr, independently of the star formation timescale, carbon stars with lower initial masses and correspondingly longer carbon rich lifetimes accumulate. In the meantime the star formation timescale sets the rate of increase of the interstellar [Fe/H].

For older stellar systems that have reached the quasi-stationary regime of carbon star production, the normalized number of carbon stars remains constant over a wide range in metallicity, up to solar. This is the case for the same reasons invoked above to interpret the insensitivity of the mean bolometric luminosity to the metallicity. Over this range in metallicity, chemically consistent evolutionary

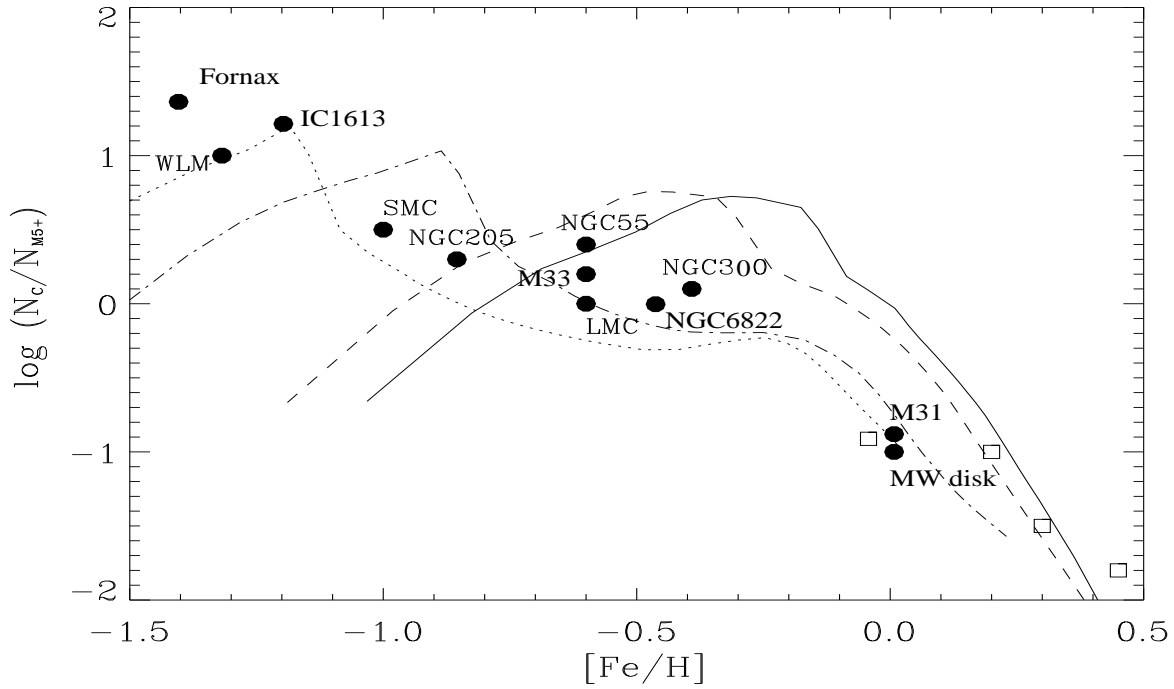


Figure 8. The logarithmic ratio of the number carbon stars to the number of late M-type stars, as a function of the metallicity of the host galaxy (gas phase). The chemical evolution assumed here is a closed box. Different lines refer to different star formation histories. For stellar populations older than about 1 Gyr, all the models merge into a common sequence. Also shown are the observational data for the Local Group galaxies from the recent compilation of Groenewegen 1999.

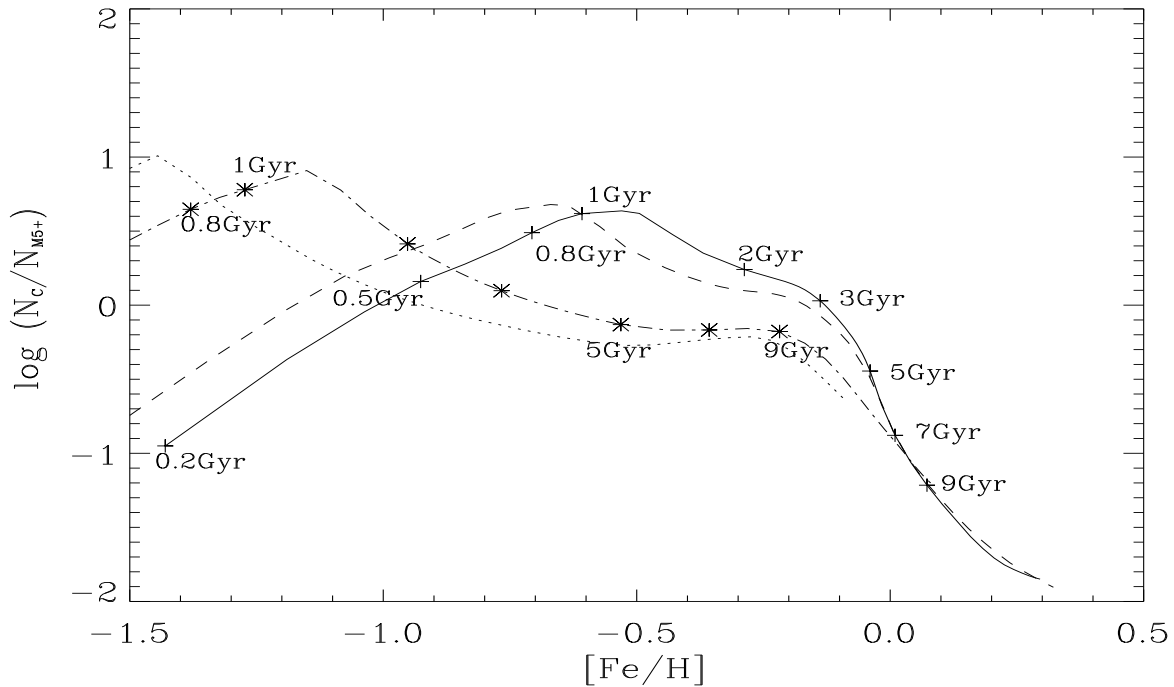


Figure 9. Same as Fig. 8, but assuming that the stellar population is formed by gas infall (see text). Also shown are a sample of ages of the considered stellar population for different star formation histories.

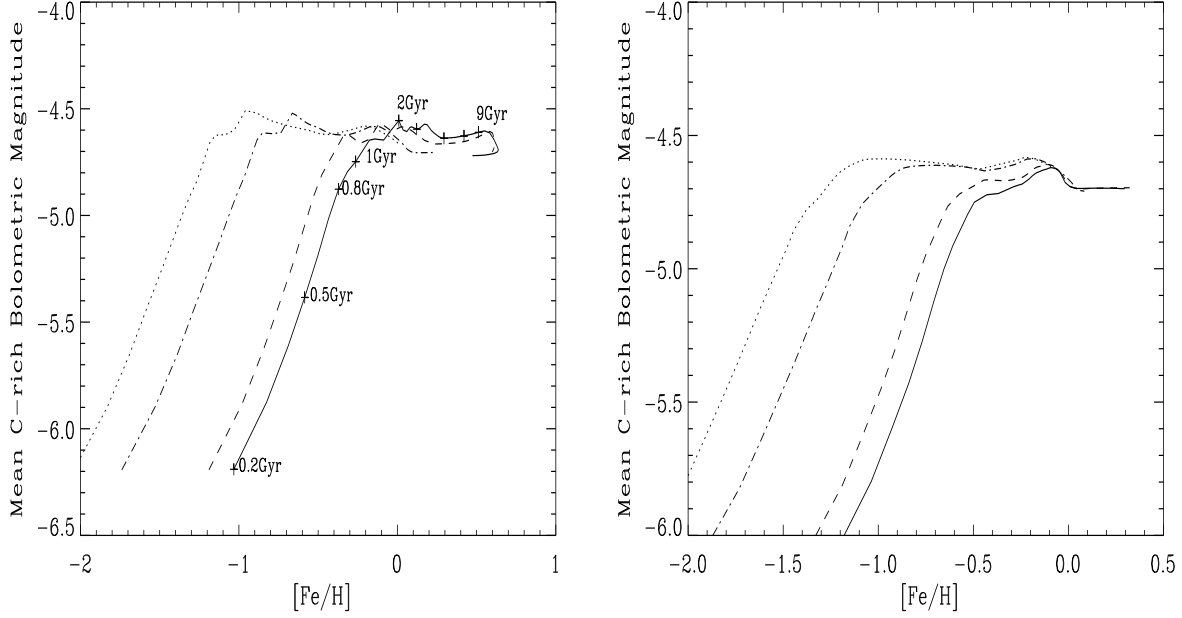


Figure 10. Left: Evolution of the mean bolometric magnitude of carbon rich stars as function of the parent stellar population metallicity assuming closed box to calculate the chemical evolution model. For stellar population older than 0.5 – 0.8 Gyr, the mean bolometric magnitude of carbon rich stars is constant for wide range of metallicity, up to solar (see text). Right: Similar to the left panel but assuming the stellar populations are formed by gas infall

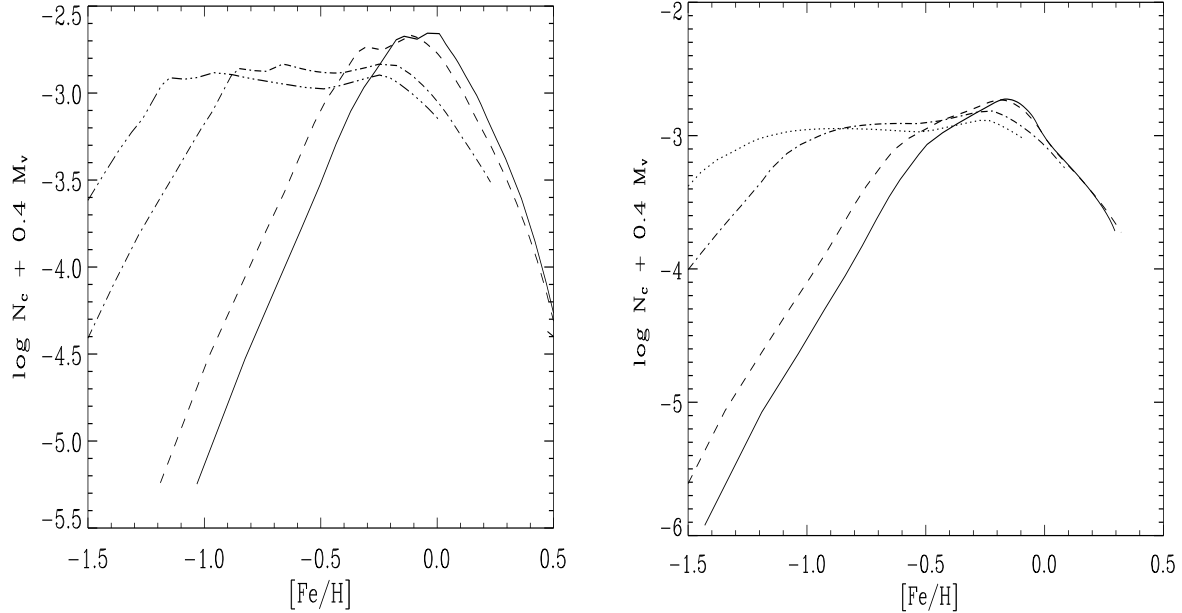


Figure 11. Left: Correlation of V-band luminosity-normalized carbon rich star number, with the metallicity for closed box model. Right: Similar to the left panel but assuming gas infall to form the stellar population.

models of stellar populations predict linear correlation between a galaxy's metallicity and its V (or B) magnitude. The plateau in both panels of Fig. 11, together with the luminosity-metallicity correlation, illustrate that the number of carbon stars is inversely proportional to $[\text{Fe}/\text{H}]$ over this range of ages, even for systems with complex star formation histories. A striking feature is that the predicted

value of $N_{C,L}$ on this plateau is again relatively independent of the star formation history. This is because the luminosity-metallicity relation is independent of the star formation history, as long as latter is continuous. The predicted average value of the normalized number of carbon star is ~ -3 . The agreement between the predicted value and the observed ones is rather good.

For old metal-rich systems (i.e. when $[\text{Fe}/\text{H}] \geq 0.$), all star formation scenarios predict that the normalized number of carbon stars declines with increasing metallicity. This results from the very low efficiency of carbon star formation in metal-rich systems and from the fact that the magnitude-metallicity relation of the galaxies is not linear any more. Additional observations are needed to obtain more constraints on the carbon star populations of metal-rich galaxies.

In summary, the details of the star formation history do not affect the systematic behavior of the predicted relation between the metallicity and the normalized number of carbon stars, as long as a quasi-stationary regime has been reached.

7 N_C/N_M AS AN ABUNDANCE INDICATOR

The above investigations of the relations between the properties of carbon star populations and the parent galaxy metallicity have lead us to highlight the relatively short time that separates the birth of the first stars from the appearance of the bulk of the carbon stars. This time is indeed short when compared to the timescales over which the average SFR varies in Hubble sequence galaxies. Therefore, for stellar systems older than ~ 1 Gyr, for which carbon star production proceeds at a quasi-stationary rate, the N_C/N_M ratio indicates metallicity rather than age.

The time delay between the production of the bulk of the carbon stars, in terms of number, and the ejection of the bulk of iron to the interstellar medium (which is related to the lifetime of SNe Ia progenitors since SNe Ia events are the main producers of iron) is also short in comparison to the star formation timescale. The difference between the initial metallicity of progenitors of carbon stars and the interstellar medium metallicity when those stars become carbon rich is not significant, except at very early times in the life of a galaxy. This means that N_C/N_M ratio measures both the metallicity of the carbon star progenitors and the present interstellar medium metallicity.

This suggests that the N_C/N_M radial profile, for stellar systems that form stars continuously, will follow the metallicity profile and both will have the same shape (i.e. slope). This statement is valid at least for stellar systems for which the evolution is not affected by processes that could trigger rapid radial mixing of the interstellar material (such as bars or merging events for example), with a timescale shorter or comparable to the timescale of the chemical evolution, and hence carbon star production. Bars or interactions could significantly alter the local composition of the interstellar medium on timescales shorter than 1 Gyr, and break the relation between this composition and N_C/N_M .

Observations supporting this results already exist in the literature. Indeed Brewer et al. (1995) have imaged five fields along the semi-major axis of M31 to derive the radial profile of N_C/N_M . Using the compilation of Pritchet et al. (1987) to calibrate the N_C/N_M vs. $[\text{Fe}/\text{H}]$ relation, and the observed N_C/N_M radial profile, they have derived the radial abundance profile along the semi-major axis of M31. They find rather reasonable agreement with the metallicity gradient observed by Blair et al. (1981, 1982) and Dennefeld & Kunth (1981) using HII regions and supernova remnants.

Using N_C/N_M as an alternative abundance indicator has interesting advantages. It enables us to investigate the chemical evolution in environments where the traditional methods are useless, for instance far out in disks where HII regions are rare, or in the halo of galaxies. The knowledge of abundance gradient at large galactic scales can be of great help to constrain models of galaxy formation.

8 SUMMARY AND CONCLUSIONS

In this paper we have provided a theoretical investigation of carbon star populations and of related statistical properties as a function of metallicity, and we have confronted these models with available observations in Local Group galaxies. To achieve this goal we have constructed evolutionary synthesis models that use a large grid of stellar evolution tracks, including the TP-AGB. The underlying TP-AGB models take into account the processes that determine the evolution of those stars in the HR diagram and establish the duration of the TP-AGB phase. To provide predictions for the nature of the cool and luminous intermediate age stellar content of stellar populations (carbon rich or oxygen rich stars, optically visible or dust-enshrouded ones), our models account explicitly for the metallicity dependence of the evolution of TP-AGB stars. We thus derive estimates of the carbon star formation efficiency and its evolution as a function of metallicity for large grid of metallicity from $Z/Z_\odot = 1/50$ to $Z/Z_\odot = 2.5$. Note that because fundamental physical processes that govern TP-AGB evolution remain poorly understood and are calibrated in the solar neighbourhood or the Magellanic Clouds, uncertainties grow when moving away from this metallicity domain.

The evolution of carbon star properties as a function of metallicity for stellar systems with continuous star formation was modeled via new chemically consistent population synthesis models. Those models use metallicity-dependent stellar yields available in the literature for massive stars, and our synthetic TP-AGB evolution models for the new metallicity-dependent yields of intermediate mass stars. The effect of SNe Ia on the chemical evolution is also included. Effect of gas infall and of the star formation history were explored.

Comparisons between predicted carbon star population statistics as a function of the metallicity of the interstellar medium and the available data show that our models are, for the first time, able to reproduce qualitatively and quantitatively the observations in the Local Group galaxies. This success supports the choices made in the inputs of the evolutionary models. The models show that the evolution of the properties of carbon star populations are established by a combination of the following effects:

- The temperature of the giant branch varies with metallicity, leading to more late type M stars with increasing metallicity.
- In metal-poor systems, dredge-up events are more efficient in producing carbon stars and carbon rich lifetimes are longer. This is due to (i) higher core masses at the onset of the TP-AGB phase and the resulting earlier onset of third dredge-up events, and (ii) longer interpulse periods leading to more violent third dredge-up events.
- The time needed for a stellar population to form the bulk of its carbon stars (~ 1 Gyr) is significantly shorter than the typical evolutionary timescale along the Hubble sequence. This means that for systems older than ~ 1 Gyr the evolution of the statistical properties of carbon star populations will merely reflect the sensitivity of the evolution of individual TP-AGB stars to metallicity.

The last effect implies that the observed statistics are mainly determined by the current metallicity. Star formation history or any other process which has a timescale longer than about 1 Gyr have no significant effects on the evolution of the statistics of carbon stars as function of metallicity. This means that the observed N_C/N_{M5+} vs. $[\text{Fe}/\text{H}]$ correlation is a metallicity sequence rather than an age sequence. Consequently, we predict that, at least for unbarred spirals or noninteracting galaxies, the radial profile of

N_C/N_{M5+} ratio will have the same slope as the radial abundance profile.

We have also given estimates on the fraction of carbon stars that may be missed in optical surveys, showing that at the age when the bulk of carbon stars are formed (~ 0.8 Gyr after the burst), only 10%-20% are dust-enshrouded. We argue that the statistics of carbon star populations will not be affected dramatically by the missed high mass-loss rate stars.

The models show that, for stellar systems older than $\sim 0.8 - 1$ Gyr, carbon star populations have the following properties:

- The mean bolometric luminosity of the carbon stars is independent of metallicity. Such a behavior over a wide range of metallicity is consistent with a long record of observational constraints discussed in the literature (Aaronson & Mould 1985, Richer et al. 1985). The value derived from our calculations is $\langle M_{Bol,C} \rangle = -4.7$. Carbon stars can be considered as potential distance indicators.
- The number of carbon stars normalized to the luminosity of the parent stellar system is independent of metallicity over a wide range in abundance. This behavior supports the interpretation of the anti-correlation between N_C/N_{M5+} and $[Fe/H]$ as due, partially, to more efficient carbon star formation at lower metallicity. The value derived from our calculations is $\log(N_{C,L}) \simeq -3$. This is consistent with the observational constraints discussed recently by Azzopardi et al. (1999), where the authors report that the observed value is independent of metallicity and dispersed around -3.3 .

We note that our models were able to reproduce the observed statistics considering only the carbon stars formed via the third dredge-up channel, which means that faint, dwarf carbon stars will represent a small number fraction of the whole population of carbon stars.

9 ACKNOWLEDGMENTS

We are particularly grateful to J. Köppen, for helpful interactions and enlightening discussions reg. chemical evolution.

REFERENCES

- Aaronson M., Mould J., 1980, ApJ 240, 804
 Aaronson M., Mould J., 1985, ApJ 290, 191
 Aaronson M., Liebert J., Stocke J., 1982, ApJ 254, 507
 Aaronson M., Mould J., Cook K.H., 1985a, ApJ 291, L41
 Aaronson M., Olszewski E.W., Hodge P.W., 1983, ApJ 267, 271
 Aaronson M., Olszewski E.W., 1987, AJ, 94, 657
 Aaronson M., Gordon G., Mould J., Olszewski E.W., Suntzeff N., 1985b, ApJ 296, L7
 Aaronson M., Da Costa G.A., Hartigan P., Mould J.R., Norris J., Stockman H.S., 1984, ApJ 277, L9
 Albert L., Demers S., Kunkel W.E., 2000, AJ, 119, 2780
 Azzopardi M., Lequeux J., Westerlund B.E., 1985, A&A 144, 388
 Azzopardi M., Lequeux J., Westerlund B.E., 1986, A&A 161, 232
 Azzopardi M., Lequeux J., 1992, in: IAU symposium 149, *The Stellar Populations of Galaxies*.
 Azzopardi M., Breysacher J., Muratorio G., Westerlund B.E., 1998, in: IAU symposium 192, *Stellar populations in the local group*.
 Azzopardi M., 2000, in: IAU symposium 177, *Carbon star phenonemon*.
 Barnbaum C., Stone, R.P.S., Keenan P.C., 1996, ApJS, 105, 419
 Bessell M.S., Brett J.M., Wood P.R., Scholz M., 1989, A&AS 77, 1
 Blair W.P., Kirshner R.P., Chevalier R.A., 1981, ApJ 247, 879
 Blair W.P., Kirshner R.P., Chevalier R.A., 1982, ApJ 254, 50
 Blanco V.M., McCarthy M.F., Blanco B.M., 1980, ApJ 242, 938
 Blanco V.M., McCarthy M.F., 1983, AJ 88, 1442
 Blöcker T., Schönberner D., 1991, A&A, 244L, 43
 Blöcker T., 1995, A&A 297, 727
 Boothroyd A.I., Sackmann I.J., 1988, ApJ 328, 641
 Boothroyd A.I., Sackmann I.J., 1992, 1992, ApJ, 393L, 21
 Boothroyd A.I., Sackmann I.J., Wasserburg G.J., 1995, ApJ, 442L, 21
 Bowen G.H., 1988, ApJ 329, 299
 Bressan A., Fagotto F., Bertelli G., Chiosi C., 1993, A&AS, 100, 647
 Bressan A., Chiosi C., Fagotto F., 1994, ApJS 94, 63
 Bressan A., Granato G.L., Silva L., 1998, A&A 332, 135
 Brewer. J.P., Richer H.B., Crabtree D.R., 1995, AJ, 109, 2480
 Charlot S., Bruzual G.A., 1991, ApJ, 367, 126
 Cook K.H., Aaronson M., Norris J., 1986, ApJ 305, 634
 Cook K.H., Aaronson M., 1989, AJ 97, 923
 Costa. E. & Frogel. J.A., 1996, AJ, 112, 260
 Demers S., Kunkel W.E., 1979, PASP, 91, 761
 Demers S. & Battinelli P., 1999, AJ, 118, 1700
 Dennefeld M., Kunth D., 1981, AJ 86, 989
 van Eck S., & Jorissen A., 1999 A&A, 345, 127
 Evans R., van den Bergh S., McClure R.D., 1989, ApJ, 345, 752
 Fagotto F., Bressan A., Bertelli G., Chiosi C., 1994a, A&AS, 105, 29
 Fagotto F., Bressan A., Bertelli G., Chiosi C., 1994b, A&AS, 105, 39
 Fioc M., Rocca-Volmerange B., 1997, A&A, 326, 950
 Freedman W.L., Madore B.F., 1990, ApJ 365, 186
 Fritze-v. Alvensleben U., Gerhard O.E., 1994, A&A 285, 751
 Frogel J.A., Richer H.B., 1983, ApJ, 275, 84
 Frogel J.A., Mould J., Blanco V.M., 1990, ApJ, 352, 96
 Frost. C.A., Cannon. R.C., Lattanzio. J.C., Wood. P.R., Forestini. M. 1998, A&A, 332, 17
 Girardi L., Bertelli G., 1998, MNRAS, 300, 533
 Graff D.S., Gould A.P., Suntzeff N.B., Schommer R.A., Hardy E., 2000, ApJ 540, 211
 Greggio L., Renzini A., 1983, A&A 118, 217
 Green P.J., Margon B., Anderson S.F., Cook K.H., 1994, ApJ, 434, 319
 Green P.J., Margon B., 1994, ApJ, 423, 723
 Green P.J., Margon B., Anderson S.F., MacConnell D.J., 1992, ApJ, 400, 659
 Groenewegen. M. A. T., & de Jong. T., 1993, A&A, 267, 410
 Groenewegen. M. A. T., & de Jong. T., 1994, A&A, 283, 463
 Groenewegen. M. A. T., 1999, in IAU Symp. 191 Asymptotic Giant Branch Stars, ed. T. Le Bertre, A. Lèbre, & C. Waelkens (San Francisco: ASP), 535
 Guiderdoni B., Rocca-Volmerange B., 1987, A&A 186, 1
 Habing H. J., 1996, A&ARv, 7, 97
 Hardy E., Suntzeff N.B., Azzopardi M., 1989, ApJ 344, 210
 Henry R.B.C., Edmunds M.G., Köppen J., 2000, ApJ, 541, 660
 Hodge P., 1989, ARA&A, 27, 139
 Hudon J.D., Richer H.B., Pritchett C.J., Crabtree D.R., Christian C.A., Jones J., 1989, AJ 98, 1265
 Iben. I. Jr., Truran J.W., 1978, ApJ, 220, 980
 Iben. I. Jr., 1981, ApJ, 246, 278
 Iben. I. Jr., Renzini, A., 1983, ARA&A, 21, 271
 Jorissen A., Mayor M., 1992, A&A 260, 115
 Joyce R.R., 1998, AJ, 115, 2059
 Kunkel W.E., Demers S., Irwin M.J., 2000, AJ, 119, 2789
 Kunkel W.E., Irwin M.J., Demers S., 1997, A&AS, 122, 463
 Lacey C.G., Fall S.M., 1985, ApJ 290, 154
 Lancon. A., Mouhcine. M., Fioc. M., Silva. D., 1999, A&A 344L, 21
 Marigo. P., Bressan. A., Chiosi. C., 1996 a, A&A, 313, 545
 Marigo. P., Girardi L., Bressan. A., 1999, A&A., 344, 123
 Mateo, M. 1998, ARA&A, 36, 435
 Matteucci F., Francois P., 1989, MNRAS 239, 885
 Mouhcine. M., Lançon. A., 2002, A&A, in press
 Mouhcine. M., 2002, A&A, in press
 Mould J.R., Aaronson M., 1986, ApJ, 303, 10
 Nowotny W., Kerschbaum F., Schwarz H.E., Olofsson H., 2001, A&A, 367, 557

- Portinari L., Chiosi C., Bressan A., 1998, A&A 334, 505
- Pritchett. C.J., Richer. H.B., Schade. D., Crabtree. D.R., Yee. H.K.C. 1987, ApJ, 323, 79
- Rebeiro E., Azzopardi M., Westerlund B.E., 1993, A&AS 97, 603
- Renzini A., Buzzoni A., 1986, in *Spectral Evolution of Galaxies*, eds. C. Chiosi and A. Renzini, Dordrecht: Reidel, p. 195
- Renzini A., Voli M., 1981, A&A, 94, 175
- Richer H.B., Crabtree D.R., Pritchett C.J., 1984, ApJ 287, 138
- Richer H.B., Pritchett C.J., Crabtree D.R., 1985, ApJ, 298, 240
- Sandage A., 1986, A&A 161, 89
- Schönberner D. 1979, A&A, 79, 108
- Tinsley B.M., 1980, Fundam. Cosmic Phys., 5, 287
- Tout. C., Karakas. A. I., Lattanzio. J., Hurley. J. R., Pols. O. R., 1998, 1999, in IAU Symp. 191 Asymptotic Giant Branch Stars, ed. T. Le Bertre, A. Lèbre, & C. Waelkens (San Francisco: ASP), 535
- van Loon J.T., in IAU Symp. 191 Asymptotic Giant Branch Stars, ed. T. Le Bertre, A. Lèbre, & C. Waelkens (San Francisco: ASP), 535
- Wagenhuber J., Tuchman Y., 1996, A&A, 311, 509
- Wagenhuber J., Groenewegen M.A.T., 1998, A&A, 340, 183
- Wallerstein G., Knapp G.R., 1998, ARA&A, 36, 369
- Westerlund B.E., Edvardsson B., Lundgren K., 1987, A&A 178, 41
- Westerlund B.E., Azzopardi M., Breysacher J., Rebeiro E., 1991 a, A&AS, 91, 425
- Westerlund B.E., Lequeux J., Azzopardi M., Rebeiro E., 1991 b, A&A, 244, 367
- Westerlund B.E., Azzopardi M., Breysacher J., Rebeiro E., 1995, A&A, 303, 107
- Wing R. F. 1971, in Proc. of the Conference on Late-Type Stars, ed. G.W. Lockwood & H.M. Dyck (KPNO Contr. No. 554), 145
- Woosley S.E., Weaver T.A., 1995, ApJS 101, 181
- Zijlstra A.A., 1999, in IAU Symp. 191 Asymptotic Giant Branch Stars, ed. T. Le Bertre, A. Lèbre, & C. Waelkens (San Francisco: ASP), 535

This paper has been produced using the Royal Astronomical Society/Blackwell Science L^AT_EX style file.